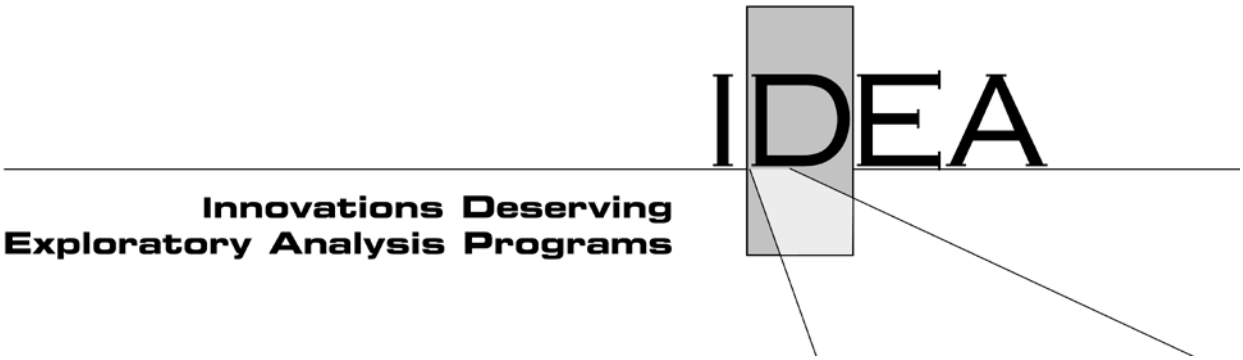

NCHRP IDEA Program

Development of an Electrical Probe for Rapid Assessment of Ground Improvement

Final Report for
NCHRP IDEA Project 186

Prepared by:
Michael A. Mooney and Richard Bearce
Colorado School of Mines, Golden CO

September 2018

TRB TRANSPORTATION RESEARCH BOARD
The National Academies of
SCIENCES · ENGINEERING · MEDICINE

Innovations Deserving Exploratory Analysis (IDEA) Programs Managed by the Transportation Research Board

This IDEA project was funded by the NCHRP IDEA Program.

The TRB currently manages the following three IDEA programs:

- The NCHRP IDEA Program, which focuses on advances in the design, construction, and maintenance of highway systems, is funded by American Association of State Highway and Transportation Officials (AASHTO) as part of the National Cooperative Highway Research Program (NCHRP).
- The Safety IDEA Program currently focuses on innovative approaches for improving railroad safety or performance. The program is currently funded by the Federal Railroad Administration (FRA). The program was previously jointly funded by the Federal Motor Carrier Safety Administration (FMCSA) and the FRA.
- The Transit IDEA Program, which supports development and testing of innovative concepts and methods for advancing transit practice, is funded by the Federal Transit Administration (FTA) as part of the Transit Cooperative Research Program (TCRP).

Management of the three IDEA programs is coordinated to promote the development and testing of innovative concepts, methods, and technologies.

For information on the IDEA programs, check the IDEA website (www.trb.org/idea). For questions, contact the IDEA programs office by telephone at (202) 334-3310.

IDEA Programs
Transportation Research Board
500 Fifth Street, NW
Washington, DC 20001

Development of an Electrical Probe for Rapid Assessment of Ground Improvement

IDEA Program Final Report

NCHRP-186

Prepared for the IDEA Program
Transportation Research Board
The National Academies

Michael A. Mooney and Richard Bearce
Colorado School of Mines, Golden CO
September 3, 2018

ACKNOWLEDGEMENTS

The authors are grateful to a number of companies for their assistance including Hayward Baker, Moretrench and Malcolm Drilling, and agencies including the Minnesota, California, Florida and Colorado Departments of Transportation for their input during this project. The authors are grateful to Max Mifkovic, a student at Colorado School of Mines for help with laboratory and field testing. Finally, the authors thank the NCHRP IDEA Program for funding the study, and Program Manager Inam Jawed and project liaison Tommy Nantung, for providing assistance throughout the investigation.

EXECUTIVE SUMMARY

This reports details the findings of the National Cooperative Highway Research Program project 186 (NCHRP-186) titled “Development of an Electrical Probe for Rapid Assessment of Ground Improvement.”

Soil improvement via jet grouting and deep soil mixing has numerous applications in transportation construction including embankment stabilization, underpinning bridge foundations and stiffening bridge approach embankments, excavation and shaft support for transit and traffic tunnels, slope stability, and creating earth retaining or hydraulic barrier walls and bottom seals. The realized geometry of the mixed ground, often called soilcrete, depends greatly on the jet grouting parameters and on the soil stratigraphy at a site. Resulting geometries are highly variable and therefore require detailed verification. The lack of rapid technologies to assess jet grout column geometries is a significant barrier. This need was the impetus for this study.

A jet grout push probe has been developed for rapid assessment of jet grout column diameter. The probe is inserted into a freshly jet grouted column immediately after removing the jet grout monitor. The test requires 20-30 minutes to collect sufficient data to estimate column diameter. The probe has been implemented on multiple jet grout construction project sites, primarily granular soil sites (sands, silty sands). In all cases, the estimated diameter was found to be within 5% of the actual constructed diameter. Extensive computational modeling was performed to provide the basis for the design and for the resistivity methodology used to determine column diameter. Continued testing of different diameter jet grout columns constructed in a variety of soil types is recommended.

In developing a plan for technology implementation, current specifications for jet grouting on transportation-related projects were examined and important consideration given to the customer for the technology, intellectual property, and the business model. Given current specifications for jet grouting, the immediate customer for the probe is the jet grout contractor community. Contractors are tasked with performing QCQA and meeting acceptance criteria. The main benefit that the probe provides over current techniques is in time savings. Instead of waiting 7 days after jet grouting to perform coring and another 7-21 days for UCS test results, a contractor can assess the diameter within 30 minutes of jet grouting. This provides immediate actionable feedback as the contractor can modify jet grouting parameters as needed within the same work shift. Further, the ability to verify diameter immediately and move on to production can save significant time and money. This ultimately benefits the owner (and tax payers) because jet grout bid prices will decrease.

The suggested business model for push probe implementation involves the university licensing the technology to one or a select group of testing companies. These companies, with well trained personnel, should carry out the testing for contractors. There is ample precedent for this in transportation construction.

TABLE OF CONTENTS

INTRODUCTION

Soil improvement via jet grouting and deep soil mixing has numerous applications in transportation construction including embankment stabilization, underpinning bridge foundations and stiffening bridge approach embankments, excavation and shaft support for transit and traffic tunnels, slope stability, and creating earth retaining or hydraulic barrier walls and bottom seals (Figure 1). Construction of jet grout columns is an involved process wherein grout (cement/water mix) is sprayed through a rotating nozzle at the end of a drill string and mixed with eroded soil in the subsurface. This process results in a column of soilcrete (soil/grout mixes) that increases the strength, reduces the deformation and reduces the hydraulic permeability of the treated soil.

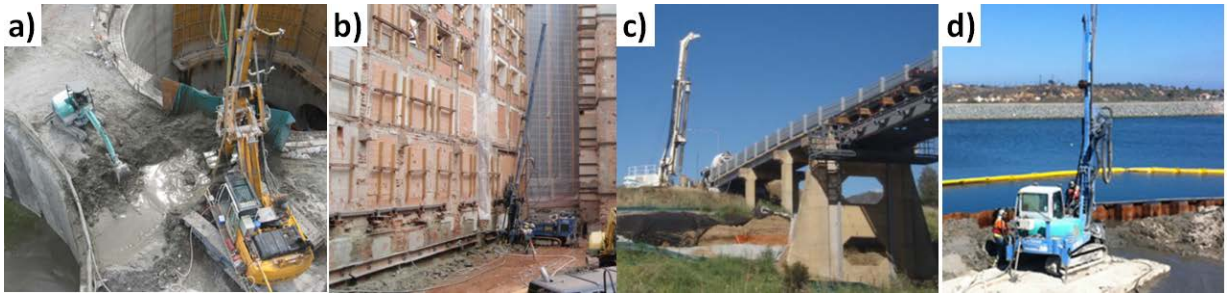

Figure 1: Jet grouting for (a) tunnel inlet/outlet, (b) underpinning urban building foundations, (c) repairing a bridge foundation, and (d) creating a hydraulic barrier wall.

To perform adequately, a jet grout column must be well-mixed throughout the entire length and cross section, and have a reasonably well known circular geometry (to match with design). In the case of an axial foundation element, the design capacity is based on an assumed diameter (see Figure 2). In the case of a hydraulic barrier wall or bottom seal, the diameter must be such that adjacent jet grout columns are contiguous and absent of voids that would permit groundwater inflow.

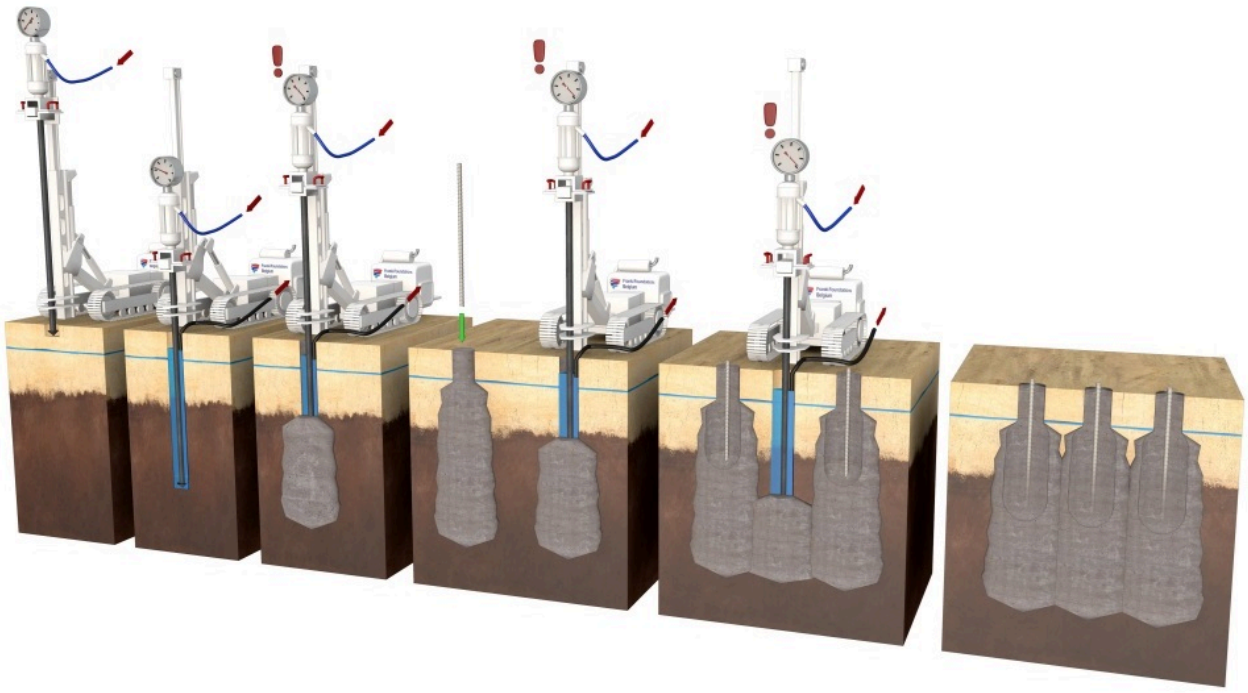

Figure 2: Jet grout construction methodology with single jet grout piles and jet grout walls (Source Franki Foundations http://www.ffgb.be/Home.aspx)

The realized jet grout column diameter is a function of the jet grout rig and jet grouting equipment parameters (fluid pressures, rotation speeds, pull out rates) and the in-situ ground conditions. Figure 3 shows a variety of exhumed jet grout columns in various soils. In all these cases, the design diameter was constant with depth. As shown however, the diameter varies, sometimes considerably.

Figure 3: Various realized jet grout diameters observed upon exhumation.

Given the importance of achieving a desired geometry combined with the variability in realized jet grout columns, jet grouting requires diligent quality control and quality assurance (QCQA) to verify they are constructed as designed. In this regard, however, there is a lack of both efficiency and effectiveness in current jet grout column QA/QC testing.

Jet grouting contractors have adopted several techniques to estimate column diameter, but these approaches have inherent limitations. Mechanical downhole devices (Passlick and Doerendahl 2006) have been employed to assess the diameter of fresh jet grout columns as has temperature monitoring (Meinhard 2002, Mullins 2010, Sellountou and Rausche 2013). Destructive tests such as radial coring/probing and column excavation can be used but require 2+ days after jet grouting for sufficient curing. Such destructive techniques are difficult to perform below the water table and can only be performed on test columns and not on production columns (e.g., Duzceer and Gokalp 2004, Yoshida 2010, Burke 2012, Bruce 2012, Wang *et al.* 2012, etc.). For verification purposes, grouting contractors often verify performance of one or more test columns and assume that the production columns constructed in the same environment will have the same geometry because the ground/grouting conditions are the same. Due to inherent geological heterogeneity and lack of precise repeatability in grouting parameters, this assumption is not always true.

Non-destructive geophysical approaches to jet grout geometry inspection have also been proposed. Mechanical wave propagation techniques including downhole/surface seismic (Madhyannapu *et al.* 2010) and crosshole sonic logging (CSL) (Niederleithinger *et al.* 2010, Bearce *et al.* 2015, Spruit *et al.* 2014) can characterize the changes in concrete/soilcrete strength (via increased wave speed), but cannot estimate geometry because the monitoring tubes are within the grouted structure. Furthermore, these methods require permanent casings and sufficient soilcrete curing time for ultrasonic/seismic wave propagation (2+ days).

Ground penetrating radar (T&A Survey 2013) and DC resistivity (Frappin and Morey 2001, Frappin 2011) have been applied to jet grout column geometry assessment, but these techniques also require a permanent casing placed in or near the column. Because these approaches all require permanent casings in or near the column, they are not feasible for rapid assessment of multiple production columns. Furthermore, the casings are not recoverable, adding an additional cost per tested column that is not efficient for evaluating production columns (as columns can number in the 10's to 100's, depending on site and application).

The existing approach for grout column geometry testing via DC resistivity (Frappin and Morey 2001, Frappin 2011) requires a permanent (water filled) slotted casing in the grout column. Electrodes submerged in water (and not directly coupled to the grout) suffer from a reduction in the accuracy with which geometry of the grout can be measured. Furthermore, the electrical protocol used in the current approach causes significant inaccuracies when subsurface anomalies (e.g., additional grout columns, utilities, etc.) are near the column (as is often the case for production columns on construction sites). This inability to adequately characterize the geometry and quality of production jet grout columns leads to premature failures, costly design, construction flaws, delayed construction, and often over-conservative construction.

An ideal approach to jet grout column inspection, and the focus of this report and study, involves the characterization of soilcrete via a recoverable push probe. This approach would provide immediate results on production columns and is truly non-destructive (i.e., no casing left in the ground and the column is not altered).

This report summarizes a new technology to achieve this, detailing the probe and the underlying physics behind the probe, describing the product design aspects of the probe as well as jobsite implementation issues, and addressing technology adoption aspects to bring such a technique into practice and widespread adoption in transportation construction.

IDEA PRODUCT

The product developed is a jet grout monitoring push probe, designed to measure the diameter with depth of jet grout columns within 30 min of jet grout construction. The probe is lowered into a freshly jet grouted column immediately after the jet grout monitor (jetting device and drill rod) is removed (see Figure 4 e). The probe uses electrical resistivity imaging to estimate the jet grout diameter. The technique, described in detail in section 3, exploits the electrical conductivity contrast between fresh soilcrete and the surrounding ground. The prototype probe is 6 m long and has ring electrodes spaced at 20-30 cm along the length of the probe. The probe is threaded together in 1.5 m long sections for shipping and portability.

The benefits that this product provides over current practice are multiple. First, the push probe test is nondestructive and rapid (currently 15-30 min). This means that production jet grout columns can be tested and not just test columns. Second, the push probe test can be performed immediately after jet grouting and while the jet grouting rig is still over the hole. This would enable the contractor to re-jet grout the hole if the results of the push probe test indicate that the diameter is not sufficient.

Figure 4: Jet grout push probe in various stages of deployment on project site. Here, the probe was lowered into a deep soil mix column with known diameter (for independent ground trothing); however, the deployment for jet grout column inspection is similar.

CONCEPT AND INNOVATION

This section explains the concept and innovation behind the jet grout monitoring push probe, and the corresponding research accomplished. The steps taken to develop and advance the probe included: (1) computational modeling to understand the capability of DC resistivity imaging with a probe and to drive electrode spacing and test protocols; (2) bench top experimentation of soil and soilcrete electrical resistivity; (3) design development and revisions to create a robust, field deployable probe; and (4) field implementation.

Electrical Resistivity Imaging

Direct current (DC) resistivity is an electrical geophysical technique that characterizes a material's electrical resistivity ρ, i.e., its ability to resist current flow. The principle behind the DC resisitivity technique is macroscopically governed by Ohm's law (Eq. 1),

$$\boldsymbol{j} = \frac{\boldsymbol{E}}{\rho} \tag{1}$$

where $\boldsymbol{j}$ is the conduction current density (A/m^2), $\boldsymbol{E}$ is the electrical field in V/m, and ρ is the material's electrical resistivity (Ωm). The electric field is defined in Eq. 2 as the gradient of the electrical potential ψ (V).

$$\boldsymbol{E} = -\nabla\psi \tag{2}$$

With the push probe, electrical resistivity measurements are carried out using a classical four electrode *A*, *B*, *M*, and *N* configuration. The current i_{AB} (A) is injected across a pair of electrodes (*A* and *B*) to create an electric field in the ground. The electric field is sampled by measuring the potential difference ψ_{MN} (V) across two measurement electrodes (*M* and *N*) of known separation distance. Using a series of measurements at various electrode spacings (e.g., Figure 5), DC resistivity can identify boundaries between materials with different resistivity.

Each measurement yields a value of resistance *R* (Ω) that is converted to an apparent resistivity ρ_a (Ωm) using a geometric correction factor *k* (m),

$$\rho_a = \left(\frac{\psi_{MN}}{i_{AB}}\right) \cdot k = R \cdot k \tag{3}$$

Each measurement corresponds to ρ_a at the midpoint depth of electrodes *M* and *N*. While the name implies that direct current is used to perform the DC resistivity test, sustained direct current can cause material polarizations that change the electrical properties of the material and therefore influences the measurement. For this reason, DC resistivity measurements are often performed using square-wave alternating current or low frequency alternating current (AC) to assess the real component of the material's resistivity.

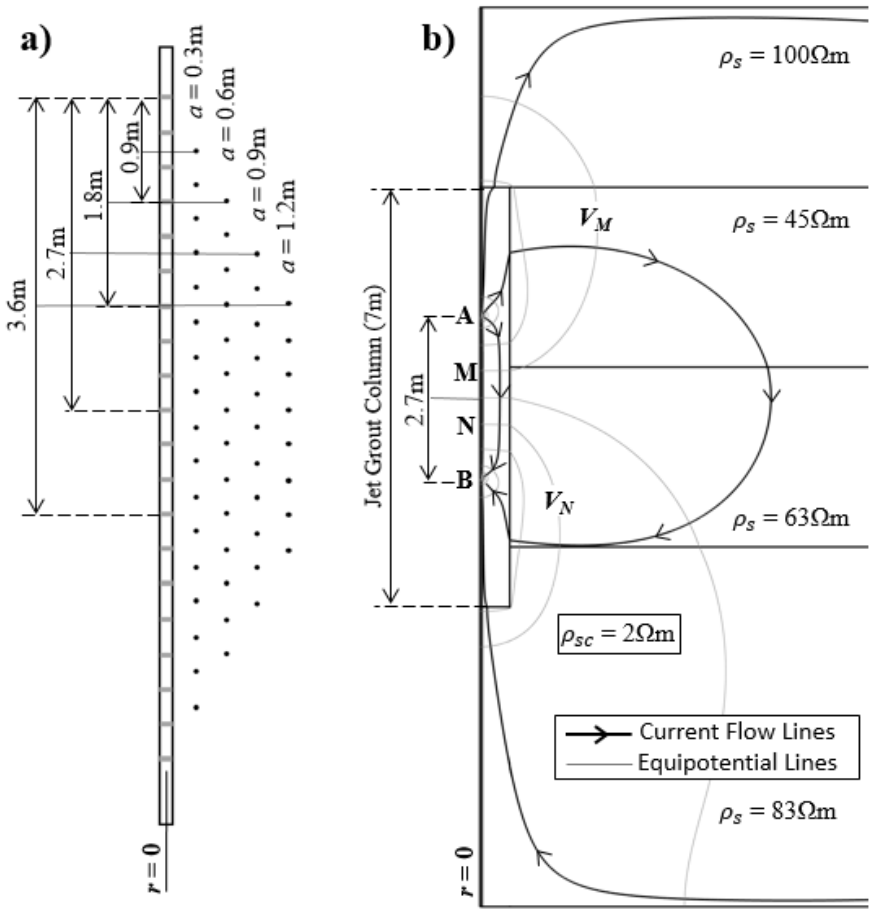

Figure 5: (a) Illustration of the 20 electrode push probe with corresponding data points for a full protocol. An example array length (3*a*) is illustrated for each value of *a* using the top electrode as injection electrode *A*. (b) An illustration of column 1 and the current/equipotential lines resulting from an *a* = 0.9m measurement.

The ρ_a obtained from DC resistivity measurements (Eq. 3) is not equivalent to a material's constitutive resistivity ρ. ρ_a is a weighted average of all ρ in the volume of material influenced by the electrical field. For a homogeneous electrically resistive medium, $\rho = \rho_a$. In heterogeneous media, e.g., layered media, ρ_a is affected by the ρ values and geometries of all materials influenced by the injected electrical field. Profiles of ρ in hetergeneous media are often obtained by inverting $\rho_a$data from multiple potential difference measurements at various electrode spacings (Revil *et al.* 2012).

As applied to jet grout column testing, DC resistivity identifies the boundary between the low resistivity in freshly mixed soilcrete and the relatively more resistive in-situ soil. This concept is illustrated in Figure 5b for a measurement with a = 0.9 m on a 1.2 m diameter jet grout column (idealized) in stratified soil. The sharp changes in the current/equipotential lines at the soil/soilcrete boundary illustrate the measurement's sensitivity to the material interface when there is a large resistivity contrast. While soil resistivity can vary greatly depending on soil type and groundwater conditions (10s-100s of Ωm), freshly mixed soilcrete has a much lower resistivity (approximately 1.5-3Ωm) that depends on the cement type and the grout to soil ratio in the soilcrete (Bearce 2015).

The low resistivity of fresh soilcrete is due to the ionic pore fluid in the cement grout. Shortly after jet grouting, soilcrete is in a wet slurry form with highly connected pore space. This initial slurry state maximizes the porosity and the ionic concentration in the pore fluid. As curing occurs, the pore fluid ions undergo chemical reactions that form cementing compounds and bond soil grains together. As pore fluid ions are transformed in chemical reactions, the soilcrete's resistivity increases. The cementing of soil grains results in reduced/disconnected porosity and also increases the soilcrete resistivity (Rajabipour *et al.* 2007).

For the Wenner-α array used by the probe, with point electrodes on the surface of an infinite homogeneous halfspace, $k = 2\pi a$, where *a* is the distance between any two adjacent array electrodes (m). When electrodes are sufficiently deep in the ground and no surface boundary effects are present, i.e., full space conditions, $k = 4\pi a$. In practice, full space conditions apply when measurements are sufficiently deep in the ground such that no surface boundary effects are present. The near surface geometric factor transitions from half to full space conditions. The depth required to reach a full space condition is dependent on the electrode spacing, but occurs 4-8 m below ground surface for the electrode spacings used by the push probe. *k* factors for the probe are similar to halfspace conditions near the surface and full space conditions at sufficient depth (which depends on electrode spacing). The ring-shaped electrodes designed for the push probe also affect *k*. The push probe *k* factors were determined for each applicable depth and *a* value (at 0.3m intervals) using finite element (FE) modeling in Cosmol Multiphysics® (see Bearce *et al* 2018).

Potential for Spectral Induced Polarization

In addition to time domain resistivity (so called DC resistivity), frequency domain resistivity (so called spectral induced polarization, SIP) was explored as a way to improve the characterization of jet grout columns in conductive soils, e.g., clays, clayey sand, salt-water saturated sands, etc. In these soils where the conductivity contrast between soilcrete and surround ground is low, DC resistivity will not be as effective. SIP is a frequency domain electrical method that characterizes a material's electrical resistivity and chargeability over a broad range of frequencies (1 mHz to 45 kHz in this study).

The laboratory setup for SIP measurements is shown in Figure 6. Bench top testing evaluated grouted clay and sand placed into a sample holder. Alternating current of a known frequency is injected into a specimen and the potential difference response is measured Figure 6). The potential difference response has the same frequency as the injected current, but there is a phase shift between the two responses. This phase shift (usually on the order of mrad) is plotted against the injection frequency over a range of injection frequencies.

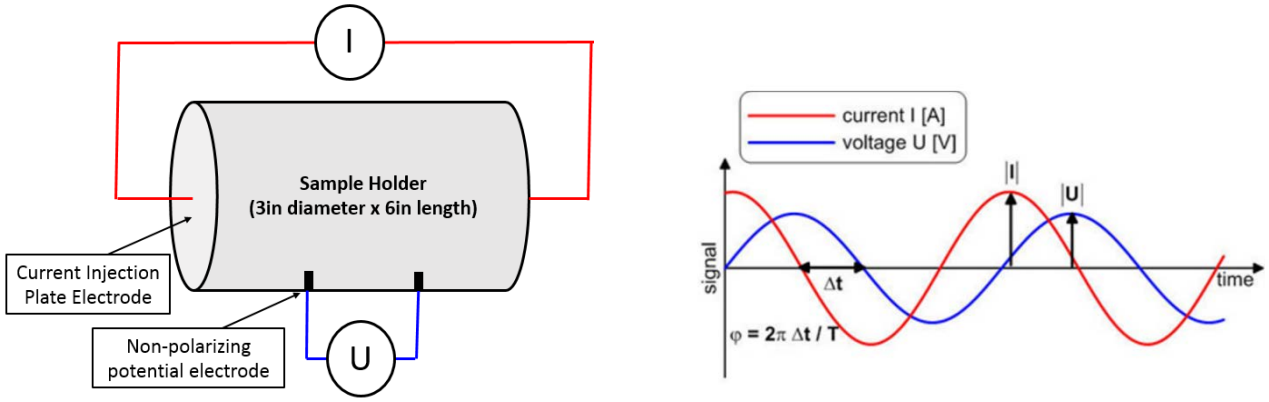

Figure 6: Testing configuration for current injection and voltage measurement for SIP testing (left); alternating current input signal and resulting measured voltage (right).

The SIP test can also provide an estimate of the material's resistivity ρ. This is helpful in comparing to the soilcrete measurements recorded by the probe with *a* electrode spacing. Electrical resistivity testing uses low frequency, e.g., 1 Hz, alternating current to estimate the resistivity of a material, and thus when evaluating a range of frequencies (via SIP), the resistivity result is also obtained. Figure 7 illustrates the problematic nature of imaging soilcrete conductive soils. In Figure 7, the resistivity of the sand is approximately 43Ωm. This is significantly more resistive than the resistivities of the soilcrete (2.8-4.1 Ωm) This resistivity contrast between the sand and the soilcrete allows the boundary between these two materials to be imaged using electrical resistivity testing. A conductive clay was also evaluated, and had a resistivity of 5 Ωm. This 5 Ωm is very similar to the resistivity of the soilcrete, making it difficult to image the boundary between the two materials using traditional resistivity testing.

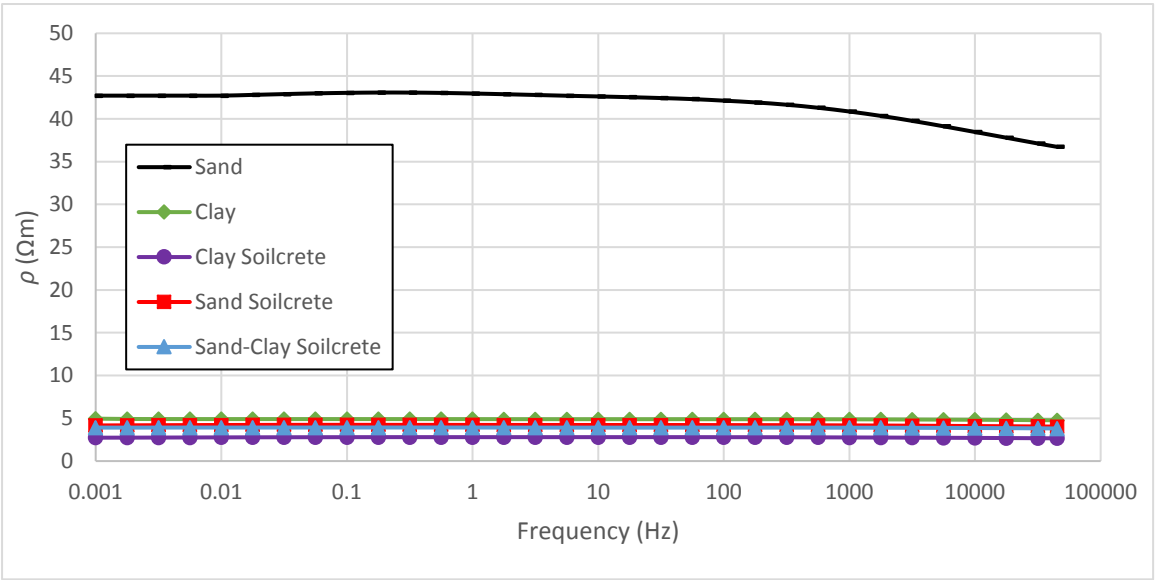

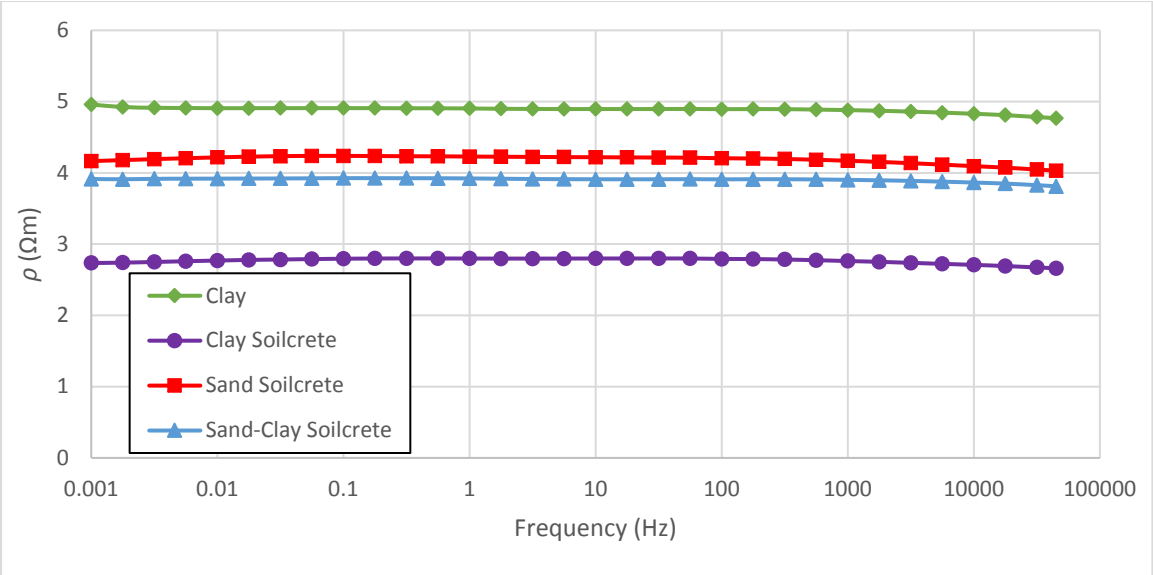

Figure 7: Electrical resistivity as a function of current injection frequency for sand, clay, clay soilcrete, sand soilcrete, and sand-clay soilcrete. Bottom plot omits the sand response.

Example SIP data from soilcrete are shown in Figure 8. Differences in phase shift as a function of frequency are related to the material polarization mechanisms that occur at different frequencies. For example, a phase shift in the mHz to Hz range often corresponds to the dominant grain size distribution in the material. Soilcrete induces significant variation in phase shift as a function of frequency. Note that the negative phase shift in Figure 8 constitutes a calibration error in the test procedure. This does not influence the relative comparison of results.

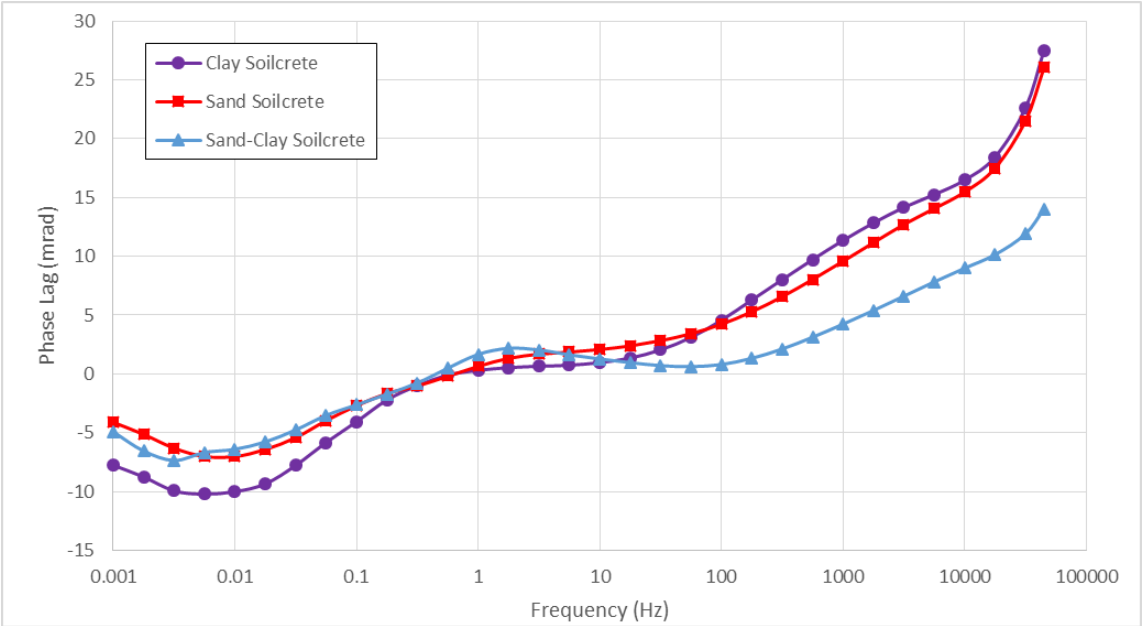

Figure 8: Phase shift between current and voltage vs. current injection frequency for clay soilcrete, sand soilcrete, and sand-clay soilcrete.

Computational Modeling to Support Design

Extensive computational modeling (via finite element analysis, FEA) was performed to evaluate different electrode spacings and injection/measurement protocols. The primary goal of this modeling was to optimize the testing procedure to maximize spatial measurement coverage and volume of current injection influence while minimizing acquisition time. For DC resistivity testing on soilcrete columns, a greater volume of current injection influence, i.e., larger spacing between the current injection electrodes, is able to estimate the diameter of larger diameter soilcrete columns.

Two protocols for current injection and electric field measurement were investigated: (1) a traditional Wenner-α protocol and (2) a gradient array protocol (shown in Figures 9 and 10). The traditional Wenner-α protocol uses a constant distance *a* between any two measurement/injection electrodes is equivalent, i.e., *AM = MN = NB*. Figure 9a illustrates the maximum *AB* usable by the probe and results in the greatest volume of current injection influence. This measurement results in only one data point (labeled in Figure 9b). This is a limitation of the Wenner-α protocol. Larger values of *AB*, and thus larger values of *MN*, lead to low resolution zones near the top and bottom of the probe (Figure 9b). For this reason, regions near the top and bottom of the probe (often corresponding to the top or bottom or soilcrete columns) may be difficult to image.

The gradient array protocol allows for larger values of *AB* with greater spatial measurement coverage near the top and bottom of the probe. The gradient array protocol (Figure 10) provides a measurement between every pair of adjacent measurement electrodes ($M_{\#}$) between the injection electrodes *A* and *B*. The gradient array's increased spatial measurement coverage (Figure 10b) eliminates the low resolution zones experience when using the Wenner-α protocol (Figure 10b), therefore providing improved resolution of the soil/soilcrete boundaries at the top and bottom of soilcrete columns. From a testing standpoint, the gradient array protocol allows the probe to evaluate larger diameter columns than the same probe with the Wenner-α protocol. Depending on the measurement device capability to accept simultaneous measurements, this can provide more rapid inspection.

The gradient array approach also expedites the time required to run the FE forward model for column diameter estimation. With the Wenner-α approach, a single injection/measurement requires an entire stationary model run to simulate the electrical field resulting from the specified current injection. For the gradient array, a single model run can estimate every data point desired for a specified current injection. For example, the measurement configuration shown in Figure 10a (and the labeled column in 10b) would only require one stationary electrical model to simulate. Conversely, the Wenner-α approach would require 25 stationary models to simulate 25 data points.

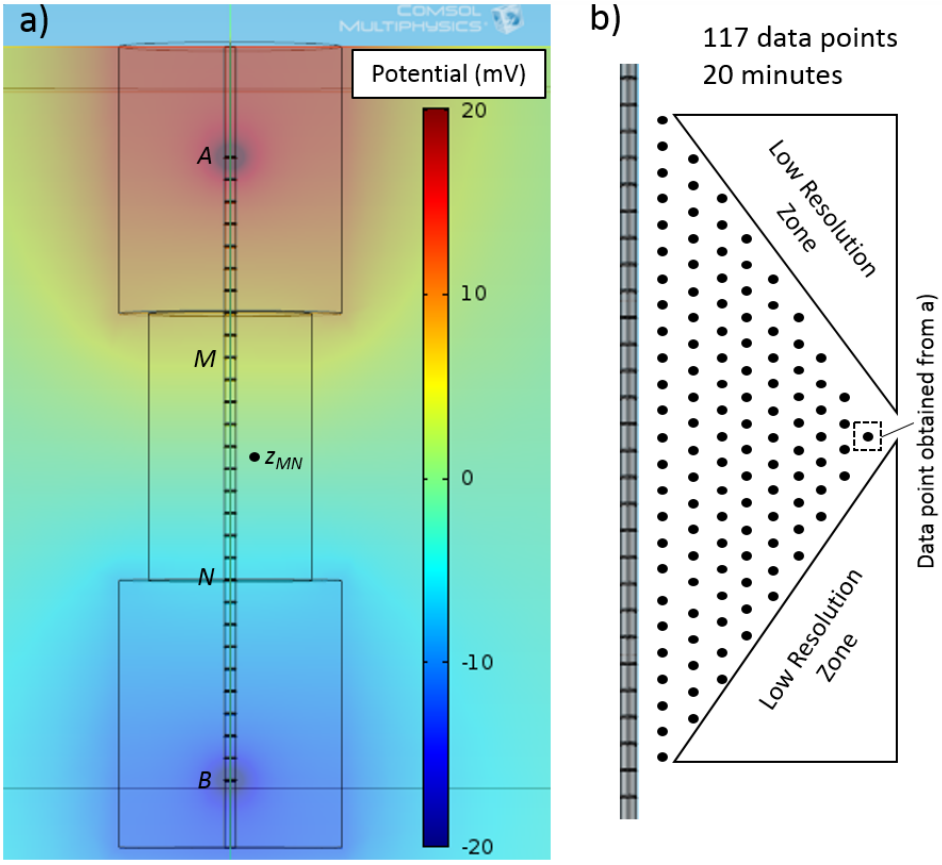

Figure 9: (a) Illustration of the Wenner-α protocol for the first generation push probe in a soilcrete column. The illustration shows the electrical field resulting from current injection across electrodes *A* and *B* and the point z_{MN} that corresponds to the depth of the measurement obtained from taking the potential difference across electrodes *M* and *N*; (b) the full data set obtained from a Wenner-α protocol using the probe.

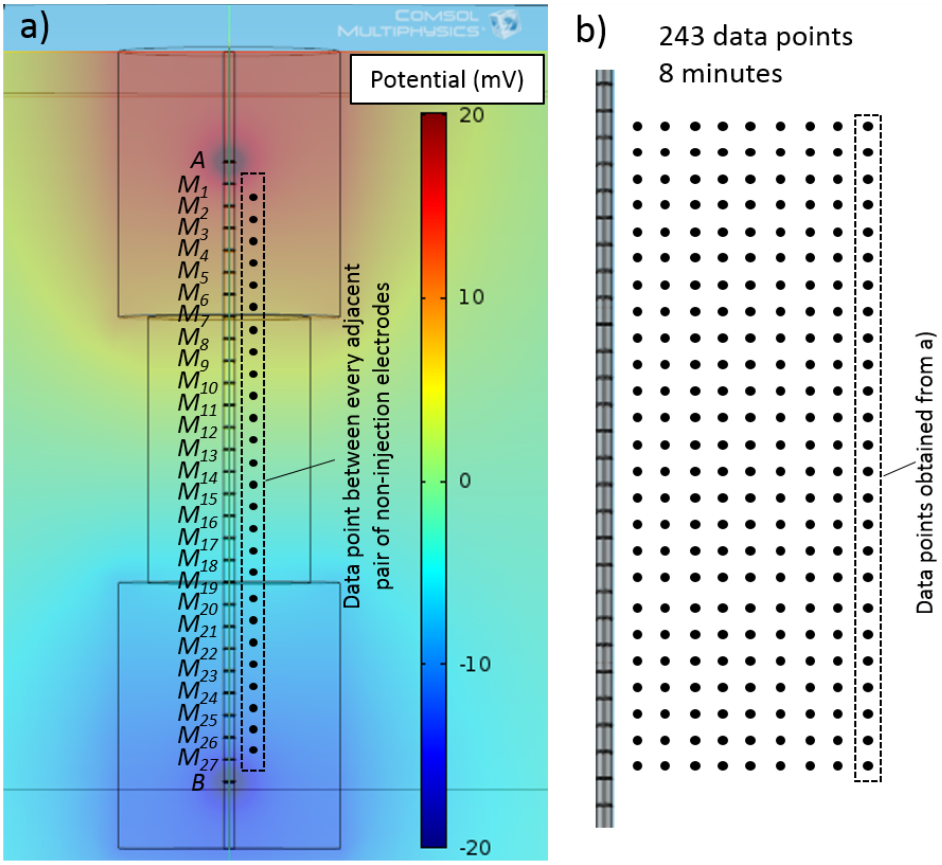

Figure 10: (a) Illustration of the gradient array protocol for the second generation push probe in a soilcrete column. The illustration shows the electrical field resulting from current injection across electrodes *A* and *B* and the multi-electrode array used to sample the potential difference across any pair of measurement ($M_{\#}$) electrodes; (b) the full data set obtained from gradient array protocol using the probe.

Based on the results of FE modeling of the gradient array, the push probe was designed with a 32 electrode configuration with 20 cm electrode spacing. This configuration results in a 6m long probe that utilizes all 32 cable connections on our data acquisition system. It is important to note that 30 cm electrode spacing is quite effective as well. The selection of electrode spacing, e.g., 20 cm vs 30 cm, is influenced by jet grout column diameter. It is clear that greater spatial resolution is achieved with 20cm spacing versus 30 cm spacing. More measurements per meter provides greater resolution. Further, the 20 cm electrode spacing can provide an in-situ estimate of soilcrete resistivity for columns with diameters greater than 1 m, while 30 cm spacing can provide an in-situ estimate of soilcrete in columns greater than 1.5 m in diameter (Bearce and Mooney 2018). Acquiring a measurement of soilcrete resistivity alone is required for diameter assessment. To this end, if jet grout columns are in the 1.0-1.5 m diameter range, a maximum electrode spacing of 20 cm is required.

In summary, computational modeling shows that a push probe with electrodes spaced at 20 cm and using the gradient array protocol can successfully image 1-4 m diameter jet grout columns. A push probe with electrodes spaced at 30 cm successfully image 1.5-3.0 m diameter jet grout columns.

Finite Element Modeling to Study Signal Magnitude

Computational modeling was also undertaken to study the relationship between injected current magnitude and measured potential in a variety of jet grout column and soil conditions. To perform this study, the push probe was modeled in jet grout columns with diameters of 1, 2, and 3 m. The jet grout has a resistivity of 2 Ωm, representative of fresh jet grout based on field tests. The soil resistivity of 10 Ωm is used in this study because lower values of soil resistivity will result in lower magnitude potential fields. Increasing the soil resistivity would result in higher magnitude potential measurements so the 10Ωm case serves as the lower limit for this study.

Current is injected from electrodes *A* and *B*, and the potential at measurements electrodes $M_1 - M_{30}$ is estimated (Figure 11) using the gradient array protocol. The injected current of 100 mA was used. Injecting larger amounts of current could be unsafe in the field. Note that in this protocol, *A* and *B* are the first and last electrode on the probe, i.e., the distance *AB* is at its maximum. Any electrodes on the probe could be used as *A* or *B*, but the maximum *AB* is of particular interest because it will result in the smallest magnitude potential field for the probe, i.e., the smaller the distance *AB*, the larger the magnitude of the potential field between *AB*. The magnitude of the potential field is smallest at the midpoint of *AB*. The probe has a minimum electrode spacing a = 19 cm, hereafter known as 1a. Greater spacings are also utilized, e.g., a = 38 cm (2a), a = 57 cm (3a), a = 76 cm (4a), etc. The magnitude of potential difference measurements increases with increased electrode spacing.

As shown in Figure 11a, the smallest potential difference, approximately 10 mV, occurs between adjacent electrode pairs M_{15}-M_{16} and M_{16}-M_{17}. This indicates that for a 1 m column, 1a electrode spacing can be used to obtain meaningful measurements. In Figure 11b, a 10mV signal can only be obtained by measuring the potential difference across electrode pairs M_{13}-M_{16} and M_{16}-M_{19}, indicating that for a 3 m diameter column, an electrode spacing of 3a would be required.

In Figure 12, the potential difference across electrode spacings 1a through 6a are plotted as a function of depth for column diameters 1m, 2m, and 3m. For each plot, the desired 10 mV threshold is labeled with a bold black line. For the 1 m column, 1a spacing is suitable at any depth. For the 2 m column, a spacing of 2a is needed to achieve a potential difference of 10 mV. The 3 m column requires a spacing of 3a to achieve a potential difference of 10 mV. As mentioned, the conditions of this study are meant to evaluate the lower limit case of the probe, i.e., maximum current injection spacing and minimum soil resistivity. Decreasing the current injection spacing and/or increasing the soil resistivity would result in larger potential differences. This analysis helps us to customize field protocols to only obtain meaningful measurements if we know the soil resistivity profile and planned column diameter prior to testing.

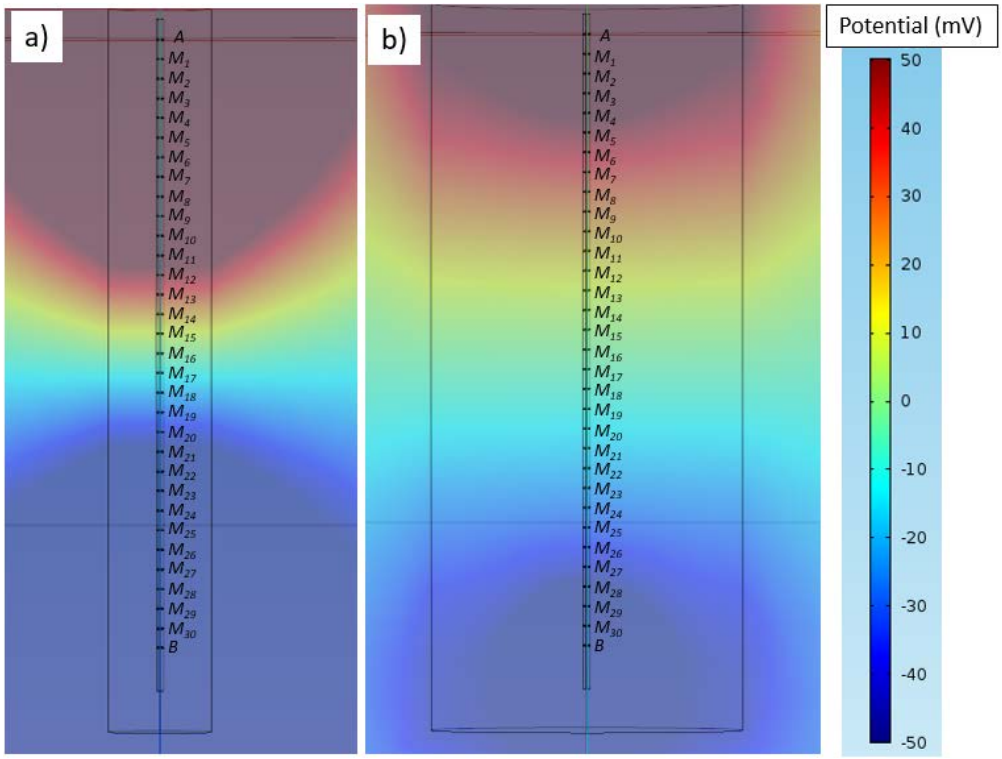

Figure 11: Potential field from 100mA current injection into (a) 1m diameter and (b) 3m diameter columns.

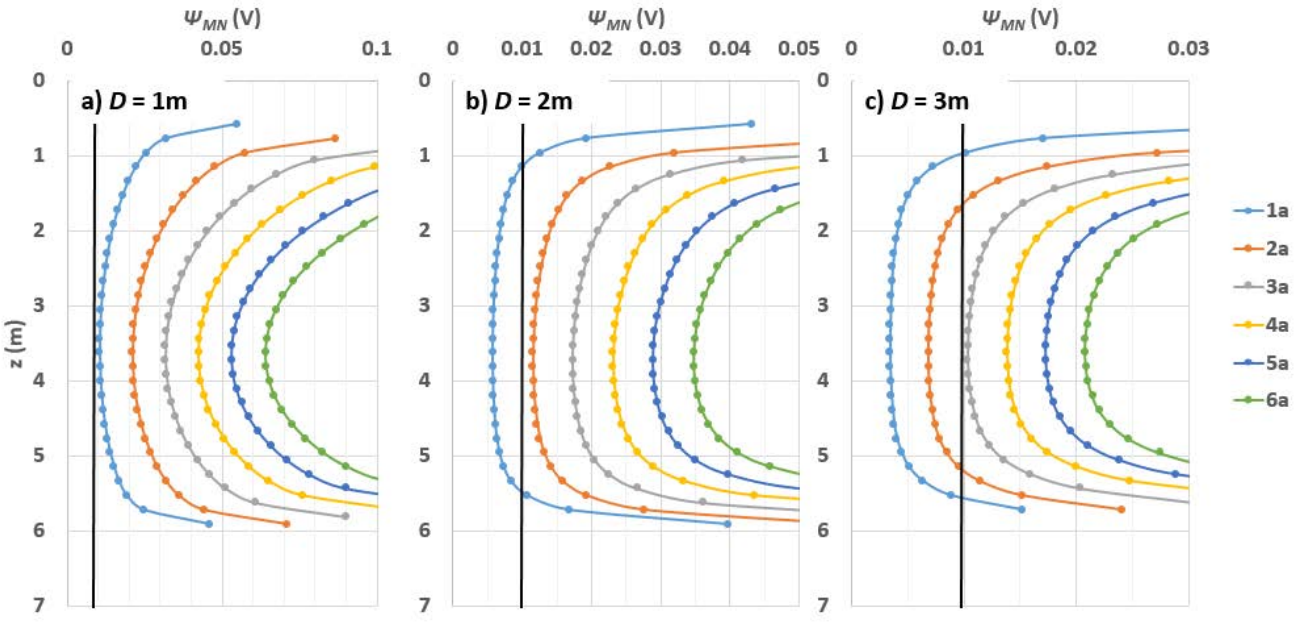

Figure 12: Potential differences estimated for electrode spacings 1*a* through 6*a* for column diameters of (a) 1m, (b) 2m, and (c) 3m.

Finite Element Modeling to Correct for Probe Inclination

FE analysis was carried out to estimate the change in probe geometric factor resulting from probe inclination. During field implementation, it is possible that the probe becomes slightly inclined. Probe inclination affects the potential field generated by the current injection and also affects the coordinates of the electrodes (Figure 13). Both of these issues may have an effect on data processing if a correction is not applied.

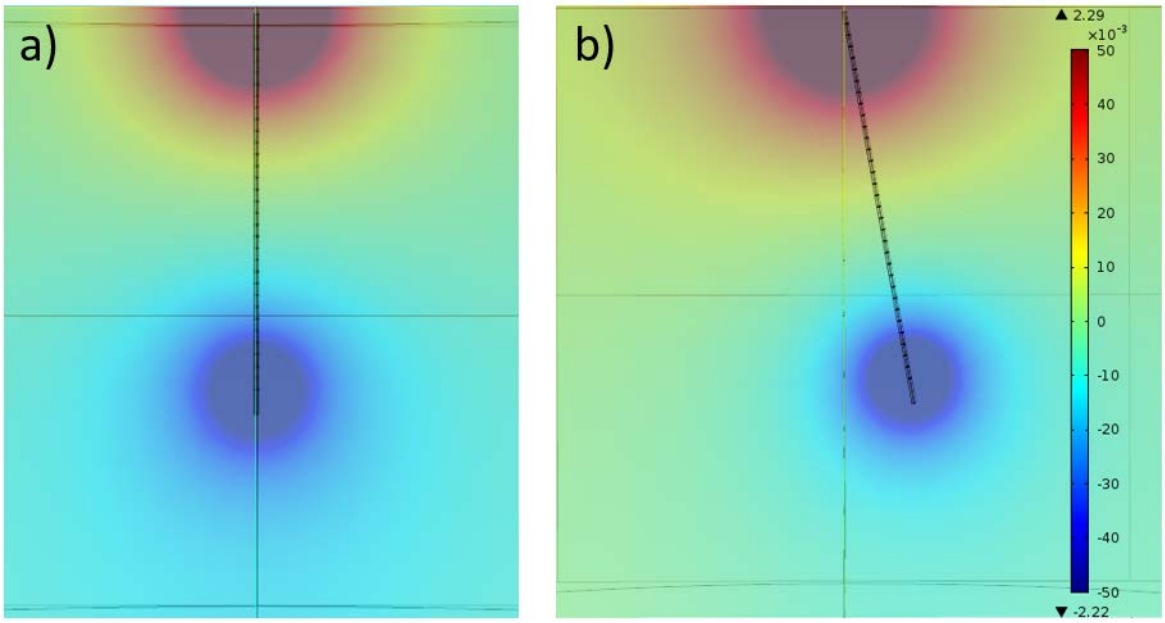

Figure 13: Potential field generated by current injection at maximum *AB* for (a) the probe in vertical position, and (b) the probe with an inclination of 10° from vertical.

In Figure 14, the geometric correction factor *k* is shown for the vertical probe and for probe inclined 10° from vertical. Figure 14b presents a zoomed in section of the global response. The difference in *k* increases with depth, and the *z* = 5m case is highlighted in Figure 14b. With an inclination of 10°, *k* at *z* = 5m is 13% smaller than *k* at the same depth for the vertical probe. The 10° inclination case is extreme. This implies that a 10° inclined probe centered at the top of a 3 m diameter jet grout column would touch the side at a depth of 6 m. Anecdotally, inclination angles on the order of 1° are more likely. The resulting error in *k* is minimal and can be neglected.

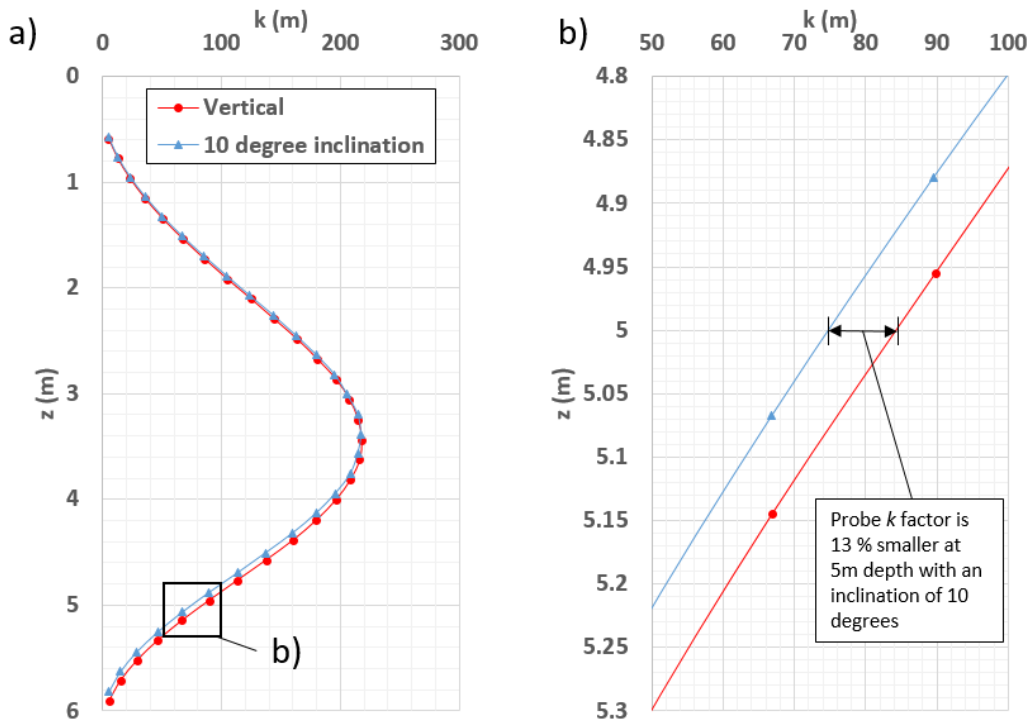

Figure 14: (a) Probe *k* factors as a function of depth for the vertical probe and the probe at 10 degree inclination, and (b) zoomed window of Figure 4a at *z* = 5m to illustrate the difference between *k* factor.

Probe Configuration

The general probe configuration involves ring electrodes sandwiched between either PVC or ultra-high molecular weight polyethylene (UHMW-PE). The configuration for the UHMW-PE probe is shown in Figure 15. UHMW-PE is desirable because it is more impact/abrasion resistant than PVC and has a lower coefficient of friction than PVC that facilitates easier insertion/removal of the probe from soilcrete.

The probe diameter shown in Figure 15 is 6.6 cm and is 6.0 m long. Ring electrodes are spaced at 20 cm. AWJ rod is used to provide stiffness and strength. A recessed pocket in the UHME-PE provides a channel for instrumentation wiring. The probe has limited internal air voids that increases the density of the probe and reduces the potential for buoyancy issues when placed in soilcrete columns. An inclinometer can be added as shown in Figure 16.

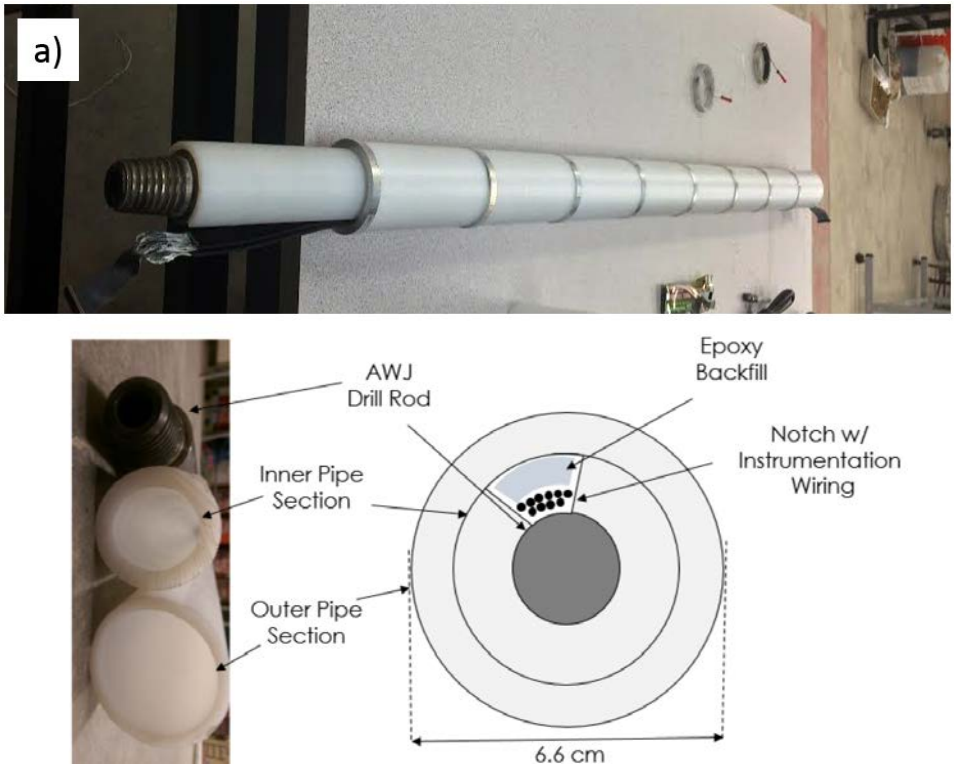

Figure 15: (a) Push probe comprised of ring electrodes sandwiched by ultra high molecular weight polyethylene (UHMW-PE). Here electrodes are spaced at 20 cm. (b) Cross section view of AWJ drill rod and UHMW-PE used in the probe.

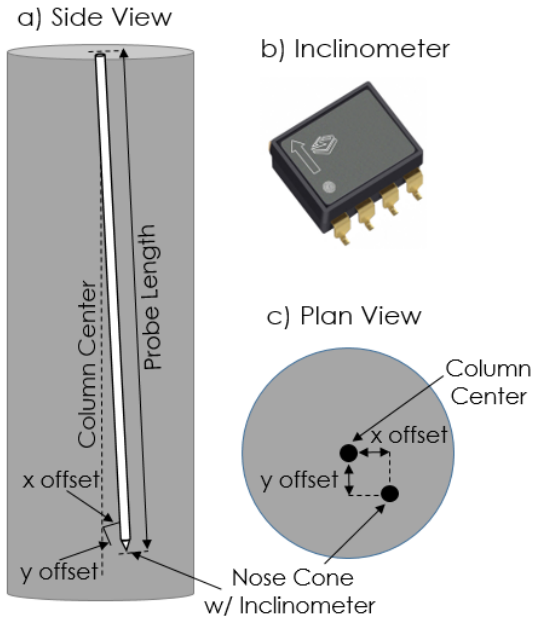

Figure 16: (a) Side view illustration of the potential x- and y- offsets encountered when placing the probe in soilcrete columns, (b) photo of the inclinometer selected for integration into the push probe, and (c) plan view of the illustration in (a).

There are multiple ways to deploy the probe on project sites. As shown in Figure 17, a portable tripod system can be straddled over a jet grout column and the probe deployed from an in-line winch. The benefit of this approach is that it does not require heavy machinery or lift equipment. The disadvantage of this approach is the time required to assemble, move and disassemble. While technically portable, a tripod system for the push probe has to be fairly significant in size (3-4 m tall). Another approach is to deploy the probe using on-site equipment as shown in Figure 17. While this does require the coordination of the contractor, such equipment seems regularly available and is much quicker to deploy and move. The benefit of the latter is that the probe can be held in one piece. Tripod use requires that the probe be assembled as it is being deployed into a jet grout column. This requires additional time. The field experience to date shows that using on-site construction equipment is the better approach.

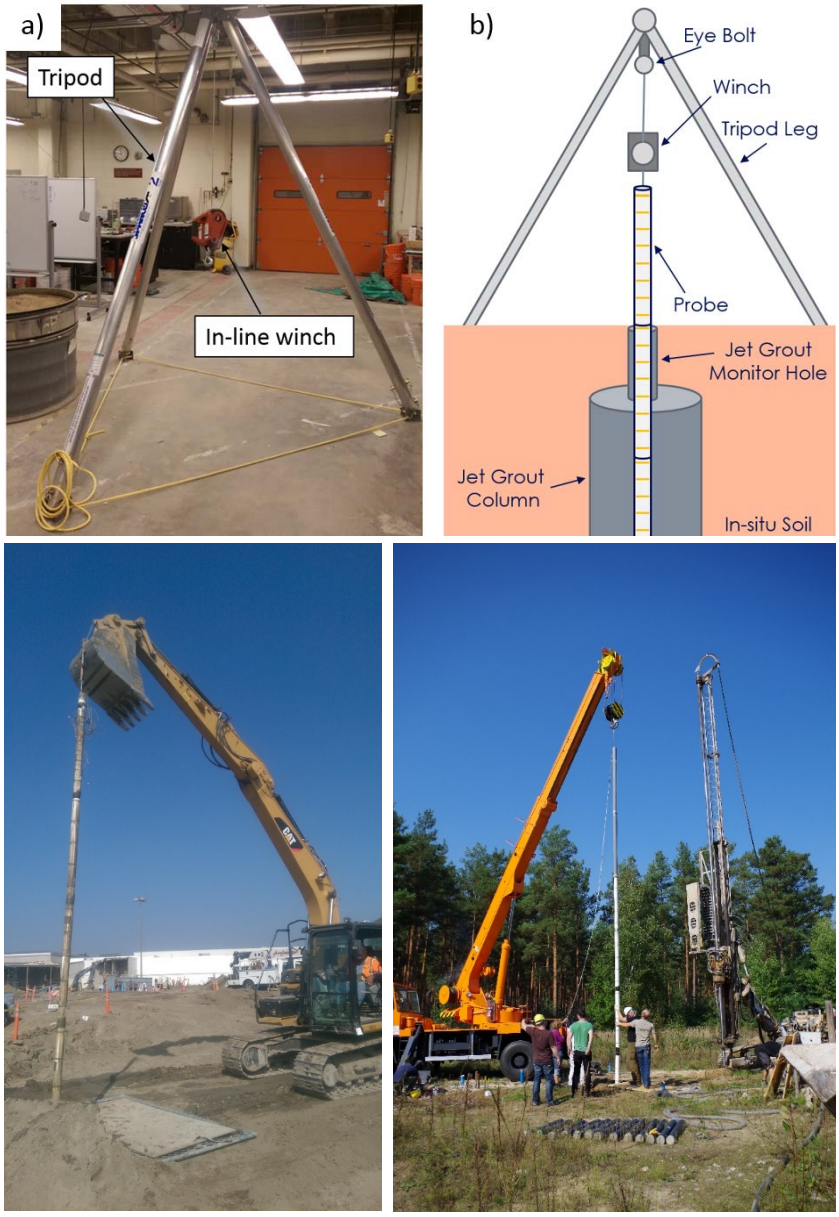

Figure 17: (top) Tripod assembly used for the deployment system; (bottom) on-site construction equipment used to deploy the push probe.

Figure 18 shows one deployment of the push probe carried out during the research project. This test was performed on a shaft bottom slab jet grout project in Hayward, California, requiring the push probe to image a jet grout column being constructed from 14 to 20 m below the ground surface. As shown in the left photograph, the probe is held vertical by a mobile crane rig and includes 14 m of dummy drill rod above the probe. This was then lowered into the hole immediately after jet grouting (right figure). The push probe is gravity fed; no down pressure is required. Once lowered to the target position, the protocol for imaging is carried out.

Figure 18: Field implementation of the probe on a jet grout project in Hayward, California. Left photo shows a mobile crane holding the probe; right photo shows the probe being lowered into a jet grouted column.

Analysis Method

The technique developed to estimate column diameter uses push probe measurements plus forward FEA results in a backcalculation approach. As shown in Figure 19a, the apparent resistivity profile for the designed-for diameter D, 0.9D and 1.1D is forward modeled with FEA. In this forward analysis, the soil resistivity ρ_s (can vary with depth) and soilcrete resistivity ρ_{sc} must be known. The former is determined through a conventional surface electrical resistivity survey; the latter is determined by the probe using a = 20-30 cm measurements.

When field measurements are obtained, as shown by the asterisks in Figure 19a, they typically lie within the 0.9D and 1.1D results (though this is not required for the analysis). The estimated diameter $\overline{D}$ is determined via linear interpolation using the FE predicted and measured values of ρ_a (Figure 19b and 19c). This approach can be done on a depth by depth basis as illustrated by the yellow and green

lines in Figure 19b and 19c. All estimated values of $\overline{D}$ can be combined to provide a diameter estimate with depth as shown in Figure 19d. Note here that $\overline{D}$ estimated from a variety of electrode spacings a reveal similar values. The average estimated diameter with depth is shown in Figure 19e. This data set was collected during testing on a deep soil mixed column with known diameter = 1.83 m. The results indicate that the estimated $\overline{D}$ is within 5% of actual.

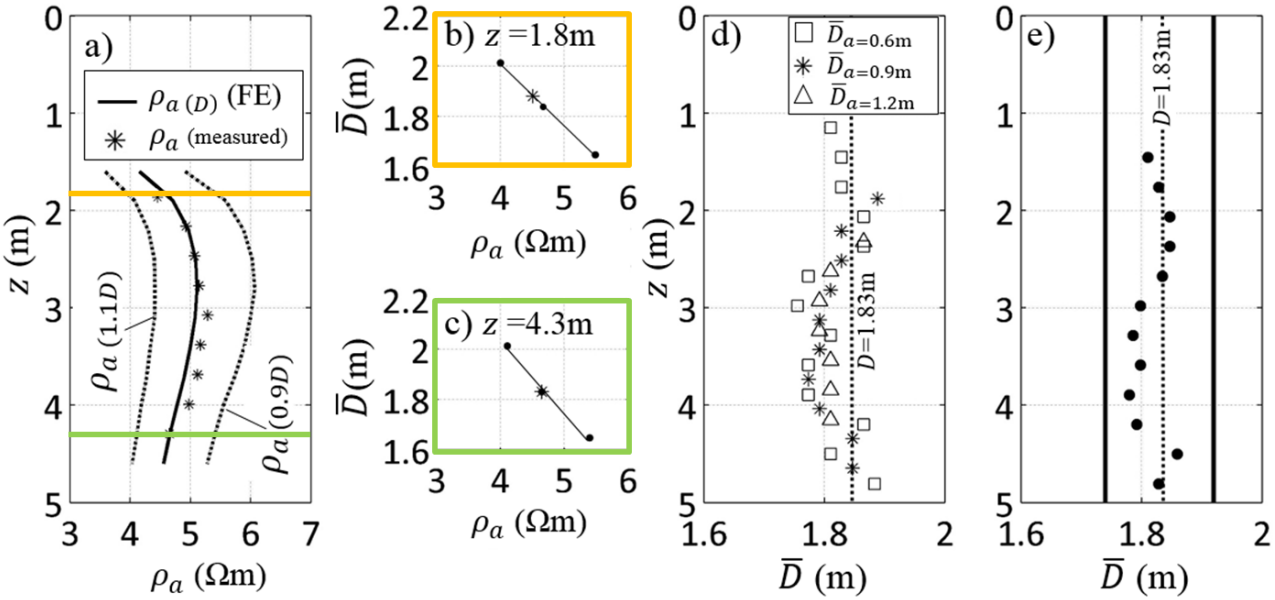

Figure 19: Summary of analysis method to estimate column diameter from electrical resistivity measurements: (a) FE analysis predicted apparent resistivity compared with probe measured; (b) and (c) linear interpolation to estimate diameter; (d) sum of all measurements; (e) average estimated diameter profile.

Diameter Assessment Results

The capabilities of the jet grout push probe is presented in this section using results from a field assessment of two jet grout columns re-analyzed as part of this study. The jet grout columns evaluated were constructed over a depth (z) range of 3-10 m (see Figure 20). The site contains post glacial sandy layers with some silts and organic materials. At the time of data acquisition, the groundwater table depth was 3 m. The estimated soil resistivity profile, measured via independent geophysical survey, is shown in Figure 20 to include 3 m of 100 Ωm dry/moist sand at the surface. Below the groundwater table, the soil resistivity decreases due to the presence of water. The best estimate of ρ_s based on field investigation shows the water saturated sand resistivity increasing gradually with depth.

Column 1 was grouted at a constant grout pressure of 40 MPa (Figure 20a), and on-site contractors estimated column 1 diameter to be between 1.2 and 1.3 m. Crosshole seismic testing performed indicated that column 1 diameter is approximately 1.25 m (Galindo-Guerreros *et al.* 2016). Column 2 was grouted at a pressure of 30 MPa from z = 3-6.5 m and 40 MPa from z = 6.5-10 m (Figure 20b). Crosshole seismic results indicate a diameter of 1.25-1.3 m from z = 6.5-7 m and a reduced column diameter of 0.9-1.1 m from z = 3-6.5 m. Immediately after jet grouting, the electrical push probe was lowered from a crane into the freshly mixed jet grout column to the depths shown in Figure 20.

Push probe measurements were acquired using a downhole variation of the traditionally surface-based Wenner-α protocol with electrode spacing a = 0.3, 0.6, 0.9, and 1.2 m. While not done during these tests, after collection of data from the probe, the probe could be lowered 2-4 m and the measurements taken again. The measurements obtained from the push probe are an axisymmetric average of the volume around the probe, and for the purpose of diameter estimation, the probe estimates an average diameter with depth.

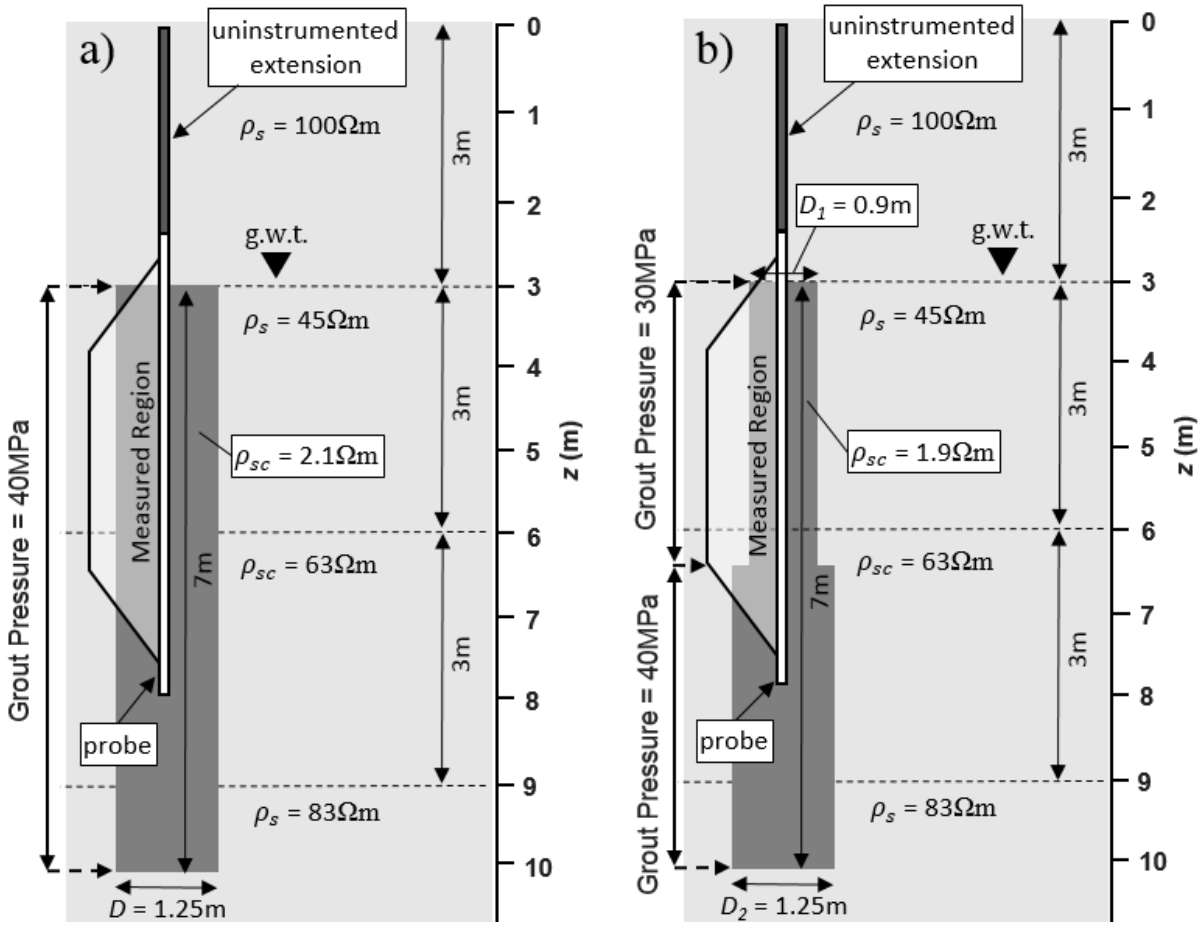

Figure 20: Soil profile, grouting parameters, probe positions, and measured region for (a) column 1, and (b) column 2.

Values of ρ_a are estimated using field-measured ψ_{MN} and i_{AB}, FE-determined k factors, and the equations presented earlier. The probe can provide an in-situ estimate of soilcrete resistivity (ρ_{sc}) for inputs to the FE model. Values of ρ_{sc} were determined from a = 0.3 m electrodes and are shown vs. depth in Figure 21. The probe experienced some electrode malfunction around 6 m depth due to a wiring issue (that was subsequently fixed). The a = 0.3 m spacing provides a good measure of the jet grout soilcrete only (no surrounding soil) for the 1.25 m diameter. However, the measurements from a = 0.3 m electrode spacing is capturing some soil response in the 0.9 m jet grout column. This is the reason for the higher ρ_a values in this area (top portion Figure 21b). The values of ρ_{sc} (2.1 and 1.9 Ωm) serve as inputs for the FE analysis required for column diameter estimation.

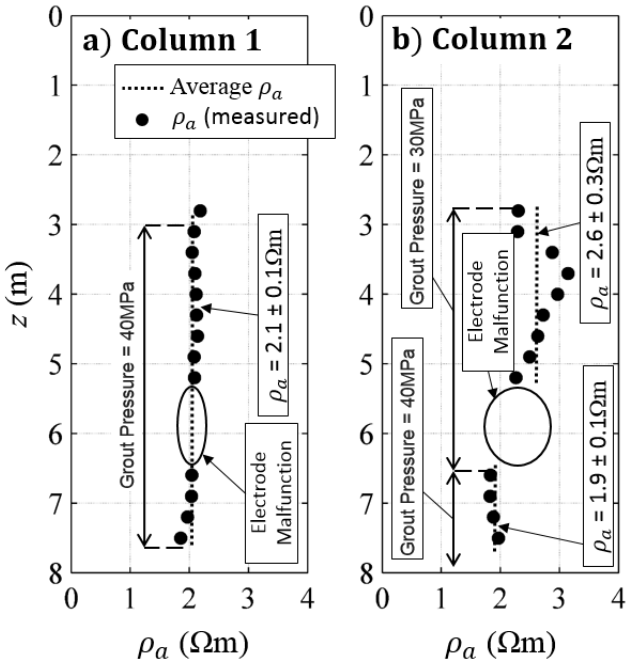

Figure 21: Experimental ρ_{sc} profiles from the a = 0.3m electrode spacing for (a) column 1, and (b) column 2.

The push probe-measured ρ_a values from a = 0.6, 0.9, and 1.2 m electrode spacings are shown for column 1 in Figure 22. The curvature of the ρ_a responses for a = 0.6, 0.9, and 1.2 m are the result of the changing soil conditions. The gradual decrease then increase between z = 3-7 m is stems from the soil resistivity profile shown in Figure 20a. The sharp change in ρ_a at z = 3 m results from the transition from in-situ soil to soilcrete column.

Also shown in Figure 22 are the FEA-modeled ρ_a profiles for D = 1.25 m, 0.9D and 1.1D. Visually, the probe-determined $\rho_a$values match closely to the FEA-modeled values for D. Using the method described in the previous section, and on a depth by depth basis, the estimated diameter $\overline{D}$ is presented in Figure 22d. These results show a constant diameter jet grout column that matches well with the contractor's estimate (based on machine parameters) and independent seismic wave testing performed days later.

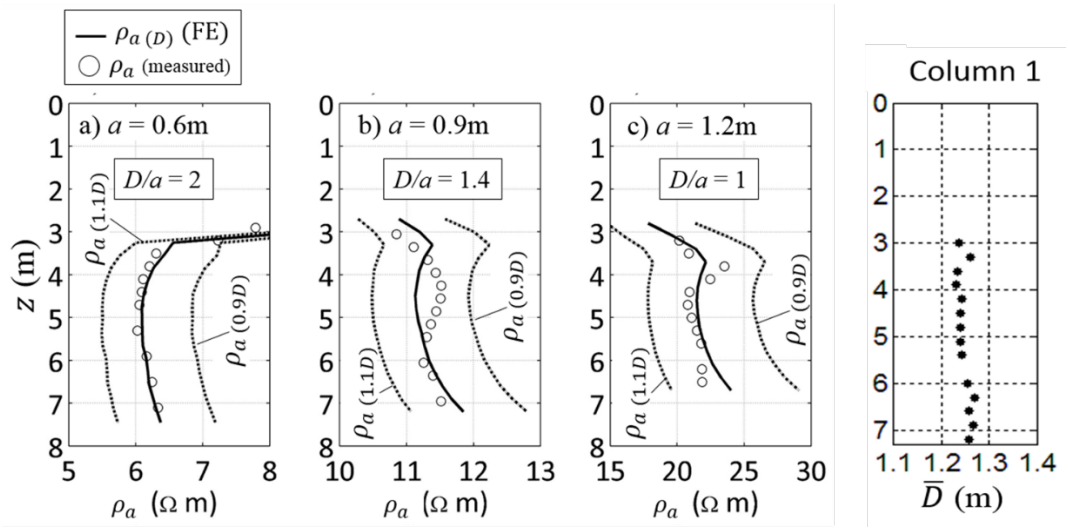

Figure 22: Experimental ρ_a responses with FE-predicted ρ_a responses for column 1 with a values of (a) 0.6m, (b) 0.9m, and (c) 1.2m. Estimated diameter in (d).

Probe-measured ρ_a for column 2 are plotted in Figure 23. In addition, FEA-modeled ρ_a responses for constant diameter and varying diameter jet grout columns are presented. The lighter gray lines show the anticipated response for constant column diameters ranging from D = 0.8 m to 1.3 m. It is clear that probe-measured ρ_a visually align with D = 0.9 m at the top of the jet grout column and with D = 1.2 – 1.3 m at the bottom of the column.

The dark solid line shows the FEA-modeled ρ_a profile for the as-built 0.9 m and 1.25 m diameter combination jet grout column. The dashed lines show the FEA-modeled ρ_a for 90% and 110% of this. A visual assessment of these figures show that the abrupt change in column diameter, from 0.9 m to 1.25 m at z = 6.5 m, yields a gradual decrease in ρ_a. The ρ_a response is not abrupt. Nevertheless, the gradual change in probe-measured ρ_a values follow the FEA-predicted response fairly well. Using the method described in the previous section, the estimated column diameter $\overline{D}$ is shown in Figure 23d. These results match well with both the contractor's estimated diameter and independent seismic wave testing performed days after jet grout column construction.

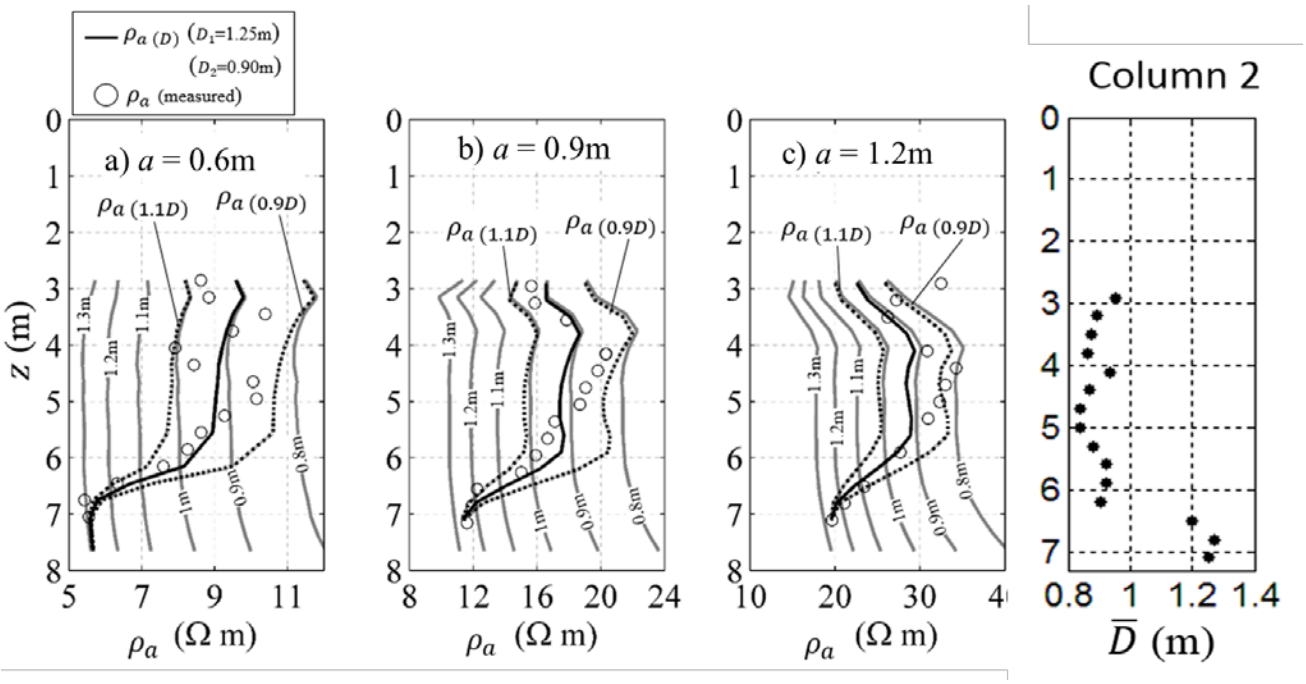

Figure 23: Experimental ρ_a responses with FE-predicted ρ_a responses (from both constant and variable diameter columns) for column 2 with (a) 0.6m, (b) 0.9m, and (c) 1.2m. Estimated diameter in (d).

In summary, the implementation of the push probe on two jet grout columns was successful in that the probe-estimated diameters were within 5% of the independently estimated (as built) diameters.

PLANS FOR IMPLEMENTATION

A number of important aspects must be addressed when considering push probe implementation. These include (1) current and typical specifications for jet grouting on transportation-related projects; (2) the customer for the technology; (3) intellectual property; and (4) the business model. These are addressed in this section.

Specifications

The specifications for transportation-related jet grouting projects typically address a variety of QC/QA requirements, verification testing and acceptance criteria. Jet grouting projects require test sections/columns so that the contractor can determine/optimize the appropriate rig parameters, grout mix composition to meet the desired column diameter. While the number and arrangement of test columns varies, verification of test columns often requires coring of hardened jet grout at the interstices of two and three columns to verify diameter. The norm is to core after at least 7 days of soilcrete curing so that the cores stay intact. Verification is based on 28-day strength tests. These assessment measures cause a significant and costly delay in moving onto the production columns.

During production jet grouting, coring is also performed periodically at interstices to assess whether the intended jet grout structure has been constructed as desired. Such coring requires hardened concrete

(at least 7 days as above) and UCS acceptance is based on meeting 28-day strength. This again requires significant amounts of time beyond the day of construction.

While UCS testing of core samples is performed by an independent laboratory, the majority of verification testing is carried out by the contractor, e.g., coring and sampling, in-situ permeability tests, wet grab sampling, etc. To this end, the contractor is the main target customer for the jet grout probe. The contractor stands to benefit the most by using the probe to immediately determine jet grout column diameter, and modify jet grouting parameters both during test phase and production as needed. The confidence gained by verifying instantly with the push probe would enable the contractor to move forward.

Long term, it is natural that jet grouting specifications will evolve with technology. For example, as the push probe or any technology gains credibility as an accurate tool, then owners will presumably see the benefit and incorporate it into specifications. Ultimately, any cost savings by eliminating waiting, etc. end up benefitting owners because bid prices will come down. Understandably, owners must be convinced of the credibility and capability of the push probe. This will require extensive proof testing with the probe on construction sites, comprehensive record keeping of capabilities, and publication of findings in peer-reviewed journals, conferences and reports. At some point, a DOT willing to take a chance will incorporate the push probe into regular or pilot specifications. When successfully performed once, then the push probe can advance at a faster rate.

Intellectual Property and Dissemination

A provisional patent application was filed by the Colorado School of Mines Office of Technology Transfer (OTT) for the jet grout push probe. The university can then license the technology to one or more companies for implementation. There are many construction monitoring devices that have followed this similar path; one being the Osterberg load cell device and test. The O-cell as it is called was invented by Professor Osterberg and colleagues, and then licensed exclusively to one company. Importantly, this company traveled to job sites and performed all tests themselves. They did not sell the O-cell separate from their services nor did they allow others to perform the test. They determined that the great care in implementation of the O-cell, conduct of the test, and presentation / interpretation of the results was vital to the success of the device. This served them and the test well, as the O-cell is a highly respected test today.

This approach is recommended for the jet grout push probe, i.e., that it be licensed to a single or perhaps a select group of testing companies. These companies will then carry out the test using trained technicians and field personnel. This is important for the jet grout probe given the complexity associated with implementation and interpretation of the results. This approach fits well with contractor practice today. For example, many jet grout contractors subcontract QC testing of jet grout samples and conduct of CPT tests.

Finally, we will disseminate the findings of this study through conference presentations, e.g., TRB, ASCE, and through publications in journals and industry trade magazines.

CONCLUSIONS

A jet grout push probe has been developed for rapid assessment of jet grout column diameter. The probe is inserted into a freshly jet grouted column immediately after removing the jet grout monitor. The test requires 20-30 minutes to collect sufficient data to estimate column diameter. The probe has been implemented on multiple jet grout construction project sites, primarily granular soil sites (sands, silty sands). In all cases, the estimated diameter was found to be within 5% of the actual constructed diameter. Extensive computational modeling was performed to provide the basis for the design and for the resistivity methodology used to determine column diameter.

In developing a plan for technology implementation, current specifications for jet grouting on transportation-related projects were examined and important consideration given to the customer for the technology, intellectual property, and the business model. Given current specifications for jet grouting, the immediate customer for the probe is the jet grout contracting community. Contractors are tasked with performing QCQA and meeting acceptance criteria. The main benefit that the probe provides over current techniques is in time savings. Instead of waiting 7 days after jet grouting to perform coring and another 7-21 days for UCS test results, a contractor can assess the diameter within 30 minutes of jet grouting. This provides immediate actionable feedback as the contractor can modify jet grouting parameters as needed within the same work shift. Further, the ability to verify diameter immediately and move on to production can save significant time and money. This ultimately benefits the owner (and tax payers) because jet grout bid prices will decrease.

The suggested business model for push probe implementation involves the university licensing the technology to one or a select group of testing companies. These companies, with well trained personnel, should carry out the testing for contractors. There is ample precedent for this in transportation construction.

REFERENCES

ABEM (2015). ABEM Terrameter LS User's Manual. Published by MALA Geosciences.

Bearce, R., Mooney, M., and Kessouri, P. (2015). Electrical Resistivity Imaging of Laboratory Soilcrete Column Geometry. *J. Geotech. Geoenviron. Eng*., 10.1061/(ASCE)GT.1943-5606.0001404, 04015088.

Bearce, R. G. (2015). Geometry Assessment and Strength/Stiffness Monitoring of Lime and Cement Modified Soils via Characterization of Curing-Induced Property Changes Estimated from Seismic Wave Propagation Techniques and Electrical Resistivity. Doctoral Disseration. Colorado School of Mines.

Bearce, R. G. and Mooney, M. A. (2018). Direct Couple Electrical Resistivity Imaging of Freshly Constructed Soilcrete Column Diameter, J. Geotechnical & Geoenv. Engr., ASCE, in review.

Bruce, D. A., (2012). Specialty Construction Techniques for Dam and Levee Remediation. CRC Press. pp 81-91.

Burke, G. K. (2012). The State of Practice in Jet Grouting. Proceedings of the Fourth International Conference on Grouting and Deep Mixing, New Orleans, LA.

COMSOL Multiphysics® (2014). COMSOL Multiphysics® Users Guide.

Duzceer, R., and Gokalp, A. (2004). Construction and Quality Control of Jet Grouting Applications in Turkey. Third International Conference on Grouting and Ground Treatment, New Orleans, LA. Feb. 10-12, 2003

Frappin, P. (2011) CYLJET – An Innovative Method for Jet Grouting Column Diameter Measurement. First International Conference of Engineering Geophysics. Al Ain, United Arab Emirates.

Frappin, P. and Morey, J. (2001) Jet Grouted Column Diameter Measurement using the Electric Cylinder Method. Soletanche Bachy. Internal Publication.

Galindo-Guerreros, J., Mackens, S., Niederleithinger, E., and Fechner, T. (2016). Crosshole and downhole seismics: a new quality assurance tool for jet grout columns. *Near Surface Geophysics*, 14(6), 493-501.

Madhyannapu, R., Puppala, A., Nazarian, S., and Yuan, D. (2010) "Quality assessment and quality control of deep soil mixing construction for stabilizing expansive subsoils." *J. of Geotech. and Geoenv. Eng.*, January 2010, ASCE.

Meinhard, K. (2002). Sizing for Strength. *Euporean Foundations*. Summer 2002, pp. 18.

Mullins, G. (2010). Thermal Integrity Profiling of Drilled Shafts. *Journal of the Deep Foundations Institute.* Vol 4, pp 54-64.

Niederleithinger, E., Hübner, M., and Amir, J.M. (2010). Crosshole sonic logging of secant pile walls - a feasibility study. In Proceedings of the Symposium on the Application of Geophysics to Environmental and Engineering Problems (SAGEEP), Keystone, Colo. Vol. 2, pp. 685–693.

Passlick and Doerendahl (2006). Quality assurance in Jet Grouting for a deep seated slab in Amsterdam. Piling and Deep Foundations Conference, Amsterdam. 2006.

Rajabipour, F., Sant, G., and Weiss, J. (2007). Development of Electrical Conducvitity-Based Sensors for Health Monitoring of Concrete Materials. Transportation Research Board 2007 Annual Meeting CD-ROM. 16 pages.

Revil, A., Karoulis, M., Johnson, T., and Kemna, A. (2012). Review: Some low-frequency electrical methods for subsurface characterization and monitoring in hydrogeology. Hydrogeological Journal (10 Feb 2012) pp. 1-42.

Sellountou, E. A. and Rausche, F. (2013). Quality management by means of load testing and integrity testing of deep foundations. Pile Dynamics Inc., Cleveland, OH. Internal publication.

Spruit, R., van Tol, F., Broere, W., Slob, E., and Niederleithinger, N. (2014). Detection of anomalies in diaphragm walls with crosshole sonic logging. *Canadian Geotechnical Journal*, Vol. 51(4), pp. 369-380.

T&A Survey (2013). 3D Borehole Radar – Determination of Jet Grout Column Diameter. T&A Survey internal publication, Amsterdam, The Netherlands.

Wang, S., Mu, M., Chen, D., and Ren, G. (2012) Field design of Jet Grouting Parameters on Soilcrete Columns. *Applied Mechanics and Materials*, Vol 170-173, pp 3068-3071.

Yoshida, H. (2010). The progress in jet grouting in the last 10 years in the Japanese market. Proceedings of the 35th Annual Conference on Deep Foundations, Hollywood, CA.

APPENDIX: RESEARCH RESULTS

TITLE: Development of an Electrical Probe for Rapid Assessment of Ground Improvement

SUBHEAD: Through a combination of finite element modeling, prototype development and field testing, this research developed an electrical probe to assess the diameter of freshly mixed jet grout columns.

WHAT WAS THE NEED?

Soil improvement via jet grouting and deep soil mixing has numerous applications in transportation construction including embankment stabilization, underpinning bridge foundations and stiffening bridge approach embankments, excavation and shaft support for transit and traffic tunnels, slope stability, and creating earth retaining or hydraulic barrier walls and bottom seals. Construction of jet grout columns is an involved process wherein grout (cement/water mix) is sprayed through a rotating nozzle at the end of a drill string and mixed with eroded soil in the subsurface. This process results in a column of soilcrete (soil/grout mixes) that increases the strength, reduces the deformation and reduces the hydraulic permeability of the treated soil.

To perform adequately, a jet grout column must be well-mixed throughout the entire length and cross section, and have a reasonably well known circular geometry (to match with design). In the case of an axial foundation element, the design capacity is based on an assumed diameter. In the case of a hydraulic barrier wall or bottom seal, the diameter must be such that adjacent jet grout columns are contiguous and absent of voids that would permit groundwater inflow.

The realized jet grout column diameter is a function of the jet grout rig and jet grouting equipment parameters (fluid pressures, rotation speeds, pull out rates) and the in-situ ground conditions. In most cases, the as-built diameter varies with depth, sometimes considerably, and typically is different than the designed diameter.

Given the importance of achieving a desired geometry combined with the variability in realized jet grout columns, jet grouting requires diligent quality control and quality assurance (QCQA) to verify they are constructed as designed. In this regard, however, there is a lack of both efficiency and effectiveness in current jet grout column QA/QC testing. In current practice, a contractor prepares test columns that are then tested for geometry 1-2 weeks later upon hardening. The tests are destructive to the column and require extensive time. This approach is very costly. As a result of the time required and destructive nature, this testing is not performed on all production columns.

An ideal approach to jet grout column inspection, and the focus of this research, involves the characterization of soilcrete via a recoverable push probe. This approach would provide immediate results on production columns and is truly non-destructive (i.e., no casing left in the ground and the column is not altered).

WHAT WAS OUR GOAL?

Develop the supporting basis, the physical prototype, and field implementation results for a jet grout push probe for rapid assessment of jet grout column diameter.

WHAT DID WE DO?

The following was completed during the course of the research:

- Detailed literature review of jet grout construction practice, specifications for construction and techniques used to inspect jet grout columns.
- Computational modeling (finite element analysis) to support the design of the probe, specifically determining aspects of electrode spacing, current injection and potential measurement protocols, influence of inclination and off-center, signal magnitude.
- Computational modeling to support the interpretation of results, including influence of surrounding soil and layered soil resistivity on column diameter estimation, the influence of electrode spacing on soilcrete resistivity measurement, and the overall algorithm to determine diameter.
- Design and build (and improve) a prototype probe for field testing.
- Field implementation to collect data; analysis of data to assess effectiveness of probe.
- Developed a plan for implementation of the push probe into practice.

WHAT WAS THE OUTCOME?

A jet grout push probe was developed for rapid assessment of jet grout column diameter. The probe is inserted into a freshly jet grouted column immediately after removing the jet grout monitor. The test requires 20-30 minutes to collect sufficient data to estimate column diameter. The probe has been implemented on multiple jet grout construction project sites, primarily granular soil sites (sands, silty sands). In all cases, the estimated diameter was found to be within 5% of the actual constructed diameter. Extensive computational modeling was performed to provide the basis for the design and for the resistivity methodology used to determine column diameter.

Commercial implementation should follow the approach used by the Osterberg load cell that was licensed to a specific company (companies). The push probe deployment should involve highly trained field personnel to carry out each test. This will build confidence in the test and build a record of test results that can be used to further interpretation and confidence in the results.

WHAT IS THE BENEFIT?

With rapid assessment of jet grout column diameter, a contractor can immediately (within 30 min) made modifications to the column if the diameter is insufficient. In current practice, a contractor waits 1-2 weeks to find out the column diameter. The development of such a rapid and nondestructive approach allows inspection of all jet grout columns instead of just test columns as is performed in current practice.